Université Libre de Bruxelles

Modélisation des rythmes du vivant

CHIM-F-422

Repressilator and Toggle switch

Author:
Charlotte Nachtegael

Supervisor:
Didier Gonze

May 20 2016

Contents

I Deterministic simulations **2**

1 Toggle Switch **3**

1.1 The impact of parameters on bistability 3

1.1.1 α_1 and α_2 parameters 3

1.1.2 δ_1 and δ_2 parameters 5

1.1.3 The Hill coefficient or parameter n 5

1.2 IPTG, temperature and switch 6

1.2.1 IPTG effect 7

1.2.2 Temperature effect 7

1.2.3 IPTG and temperature combination 8

2 Repressilator **9**

2.1 The impact of the parameters on the oscillations 9

2.1.1 The α_1, α_2 and α_3 parameters 10

2.1.2 The α_0 parameter 11

2.1.3 The β and δ parameters 12

2.2 Effect on the period 13

2.3 IPTG effect 13

2.4 GFP expression level 14

II Stochastic simulations **16**

3 Toggle Switch **17**

3.1 The effect of the size of the system 17

3.2 Near the bistability domain 18

3.3 IPTG effect 18

4 Repressilator **20**

4.1 The effect of the size of the system 20

4.2 On the limit cycle 21

4.3 IPTG effect 21

Part I

Deterministic simulations

1 Toggle Switch

The equations are based on the article of Gardner et al. [2000].

$$\begin{aligned} \frac{dx}{dt} &= \alpha_1 \frac{K_1^n}{K_1^n + y^n} - \delta_1 x \\ \frac{dy}{dt} &= \alpha_2 \frac{K_2^n}{K_2^n + x^n} - \delta_2 y \end{aligned} \tag{1}$$

Default values of parameters : $\alpha_1 = \alpha_2 = 2, K_1 = K_2 = 1, n = 4, \delta_1 = \delta_2 = 1$

The network is positive, as the number of negative reactions (reactions of inhibition) is even. We observed during the simulation of basic networks that having a positive one is a condition for the bistability of a system. We will discuss of the other conditions necessary to obtain the bistability of the system and how to switch the values from one steady state to the other.

1.1 The impact of parameters on bistability

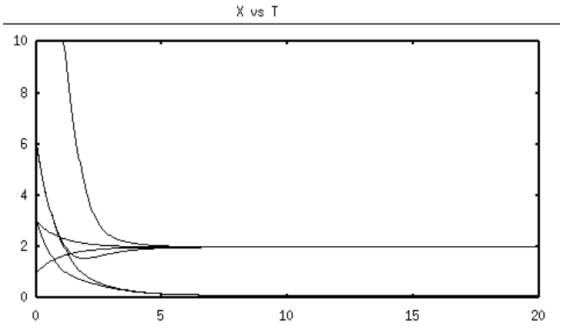

Figure 1: Simulation of the Toggle switch with default parameters and different initial conditions.

With the default parameters, we already observe a bistability of the system. Indeed, with different initial conditions, where $x_0 \neq y_0$, the curve will converge towards two different values (Fig 1). However, these parameters can be modified and consequently have an impact on the behaviour of the system.

1.1.1 α_1 and α_2 parameters

α_1 and α_2 represent the production rate of the proteins. In the article of Gardner et al. [2000], they specified that to observe bistability, you need to have high production rates. We confirmed the previous observation of the bistability by tracing the nullcline in the phase space (Fig 2a). There are three steady states : two stables and an unstable between them.

However, when we changed α_1 from 2 to 10, we observed no steady state (Fig 2b). Another phenomenon was noted with α_1 equal to 2 and α_2 equal to 1 : only one steady state, a stable node, is observed (Fig 2c).

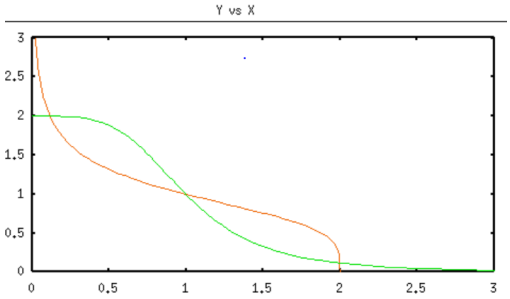

(a) Phase space with no change to α_1 or α_2

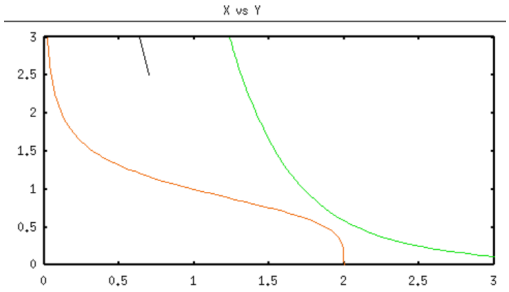

(b) Phase space with $\alpha_1 = 10$

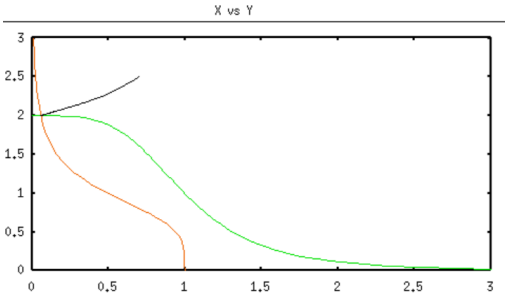

(c) Phase space with $\alpha_2 = 1$

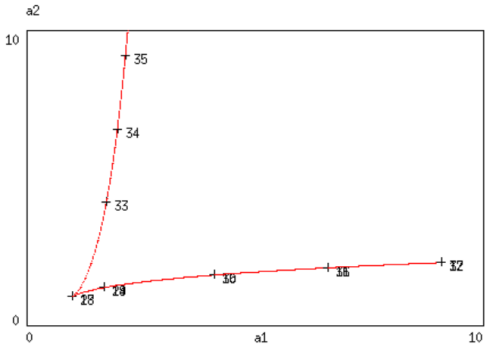

(d) Stability diagram of α_1 and α_2

Figure 2: Study of the impact of α_1 and α_2 on the behaviour of the Toggle Switch system

To further understand how the combination of α_1 and α_2 impacts on the stability of the system, we drew the stability diagram of these two parameters. Moreover, a previous study of this kind of network showed the importance of the Hill coef-

ficient (n) on the behaviour of the system, so we drew the stability diagram with $n = 4$ and $n = 2$ (Fig 2d). The bistability is obtained when we are situated within the region delimited by the red lines. This confirmed you have higher chances of bistability when you have both α with high values.

1.1.2 δ_1 and δ_2 parameters

δ_1 and δ_2 are the degradation rate of the proteins. In the paper, they are assumed to be equal. We saw in the phase space just by changing the value of δ_1 to 4 that we passed from a system with a bistability (Fig 2a) to only one stable node (Fig 3a). We drew the stability diagram for the parameters δ_1 and δ_2 and noted the region for the bistability, within the red lines, is quite small and extend only until 1,974 (Fig 3b). So we can say that δ_1 and δ_2 do not have to be both equal to 1, but that the range of their value is tight if we want the bistability.

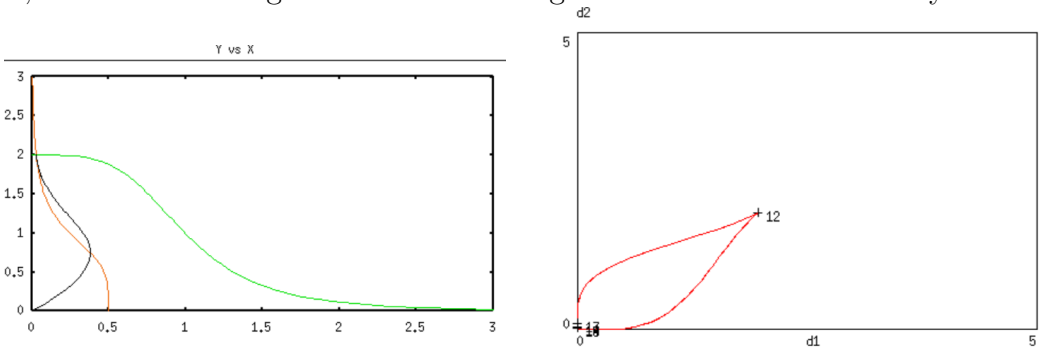

(a) Phase space with δ_1 equal to 4 (b) Stability diagram of δ_1 and δ_2

Figure 3: Study of the impact of δ_1 and δ_2 on the behaviour of the Toggle Switch system

1.1.3 The Hill coefficient or parameter n

The Hill coefficient reflects the cooperativity of the protein for the binding site. A positive Hill coefficient means that once a protein is bound to the site, its affinity for the protein increases.

The default Hill coefficient is 4 and has already been proved to be linked to bistability, as seen in the bifurcation diagram of X in function of α_1 (Fig 4a. However, if we change the coefficient to 2, we obtain only one steady state (Fig 4b).

This does not mean the system cannot be bistable, but that we need to adjust the other parameter values. Indeed, when we have $n = 2$, the region where the system is bistable is reduced as seen in the stability diagram of the parameters α (Fig 4c and 4d).

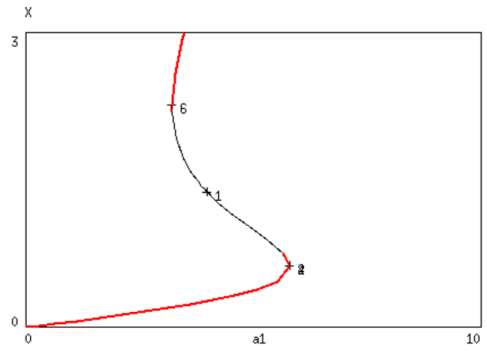

(a) Bifurcation diagram of X in function of α_1 with $n = 4$

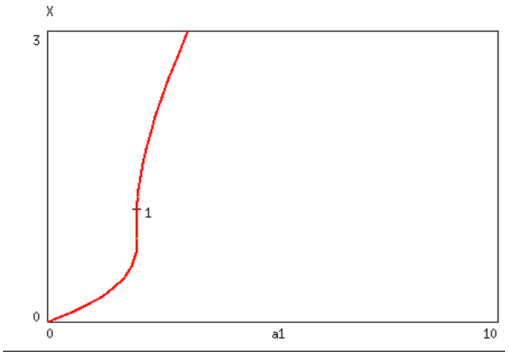

(b) Bifurcation diagram of X in function of α_1 with $n = 2$

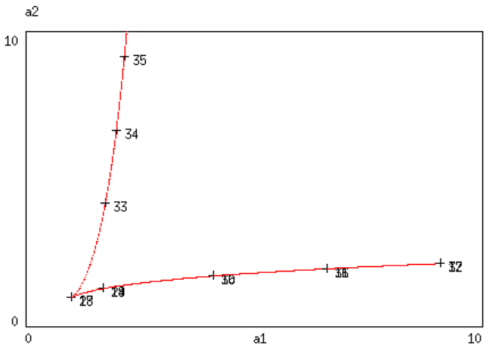

(c) Stability diagram of α_1 and α_2 with $n = 4$

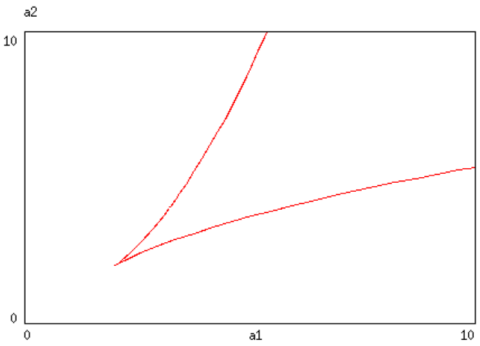

(d) Stability diagram of α_1 and α_2 with $n = 2$

Figure 4: Study of the impact of n on the behaviour of the Toggle Switch system

1.2 IPTG, temperature and switch

The compound y can be inhibited by IPTG as shown in the equation below. The other compound x is sensible to the temperature and degrades quickly in high

temperature, which is translated by an increase in δ_1

$$\frac{dx}{dt} = \alpha_1 \frac{K_1^n}{K_1^n + \left(\frac{y}{(1+S/K_s)^m}\right)^n} - \delta_1 x \qquad (2)$$
$$\frac{dy}{dt} = \alpha_2 \frac{K_2^n}{K_2^n + x^n} - \delta_2 y$$

This effects allow us to try to make the system switch between the two steady states and prove the bistability of the system.

1.2.1 IPTG effect

The bifurcation diagram of x in function of the IPTG (S) shows that two steady states are possible and that a pulse of IPTG could make the system reach the higher steady state. However, once reached, it is impossible to go back to the previous lower steady state, even by reducing the IPTG (Fig 5a). This observation is confirmed with the following simulation where a pulse of IPTG make the x compound reach the higher steady state, and the reverse for the y one, but the x does not return to its previous state after the end of the signal (FIG 5b).

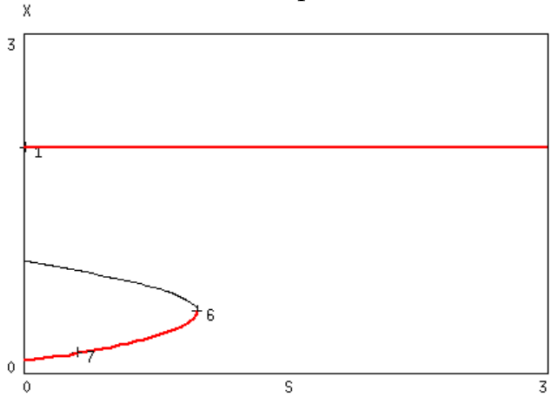

(a) Bifurcation diagram of X in function of IPTG

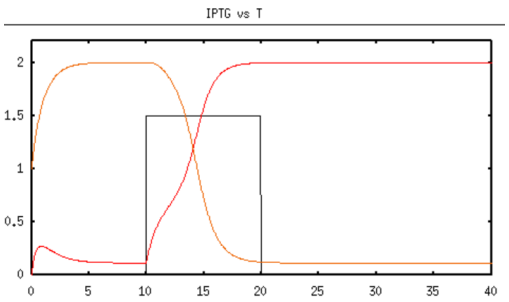

(b) Effect of a pulse of IPTG (black) on the concentration of x (red) and y (orange)

Figure 5: Switch effect with the IPTG

1.2.2 Temperature effect

To study the effect of the temperature on the system as a switch, we must initiate the system where the compound x is at the highest steady state ($x(0) > y(0)$).

When the temperature increased, increasing the degradation rate of x, we observed a switch of steady state for the compounds (Fig 6). The switch seems to be a bit faster than the IPTG switch, the former taking around 2 seconds, whereas the latter around 5.

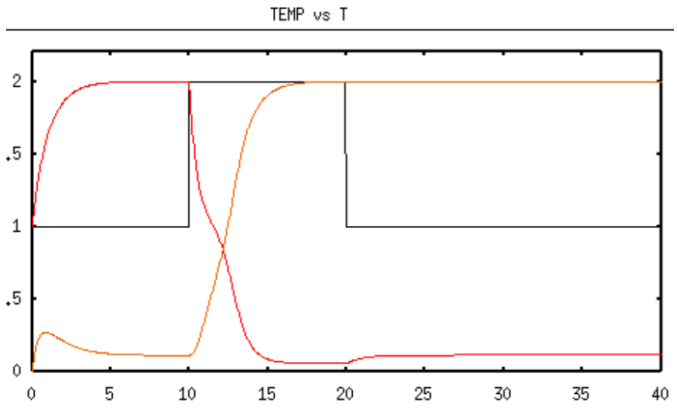

Figure 6: Effect of a pulse of temperature (black) on the concentration of x (red) and y (orange)

1.2.3 IPTG and temperature combination

Beginning with x in the lowest steady state and y in the highest, a pulse of IPTG made them switch their steady state and the following pulse of temperature made them go back (Fig 7).

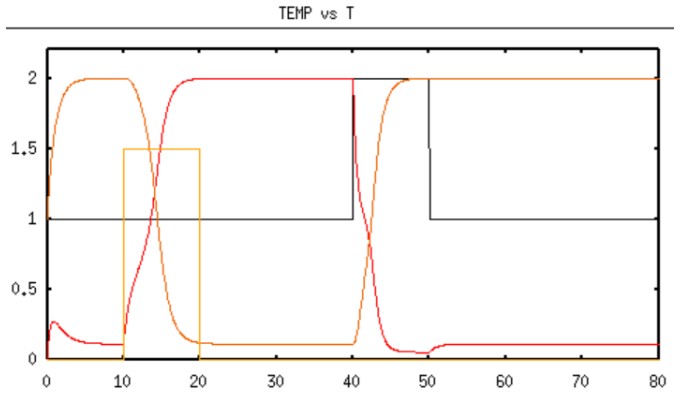

Figure 7: Effect of a pulse of IPTG (yellow) followed by a pulse of temperature (black) on the concentration of x (red) and y (orange)

2 Repressilator

The equations are based on the article of Elowitz and Leibler [2000].

$$\frac{dm_1}{dt} = \alpha_1 \frac{K_1^n}{K_1^n + p_3^n} + \alpha_0 - \gamma m_1 \tag{3}$$

$$\frac{dm_2}{dt} = \alpha_2 \frac{K_2^n}{K_2^n + p_1^n} + \alpha_0 - \gamma m_2 \tag{4}$$

$$\frac{dm_3}{dt} = \alpha_3 \frac{K_3^n}{K_3^n + p_2^n} + \alpha_0 - \gamma m_3 \tag{5}$$

$$\frac{dp_1}{dt} = \beta m_1 - \delta p_1 \tag{6}$$

$$\frac{dp_2}{dt} = \beta m_2 - \delta p_2 \tag{7}$$

$$\frac{dp_3}{dt} = \beta m_3 - \delta p_3 \tag{8}$$

Default values of parameters : $\alpha_1 = \alpha_2 = \alpha_3 = 100, \alpha_0 = 0, K_1 = K_2 = K_3 = 1, n = 2, \gamma = 1, \beta = 5, \delta = 5$

The network is negative, as the number of negatives reactions (inhibition) is odd. During the simulations of basic networks, we observed that a negative network is one condition to witness oscillations of the system. We will discuss the impact of a change of the parameters on the behaviour of the system, what happens when we integrate the IPTG as an inhibitor of one of the compound. Another topic of discussion will be to explain the curious experimental results of the paper [Elowitz and Leibler, 2000] where the average level of the GFP protein, reporter protein for the level expression of the system, tends to increase over the time.

2.1 The impact of the parameters on the oscillations

The first important thing to note is the initial conditions. If $p_1(0) = p_2(0) = p_3(0)$, the system did not produce any oscillation (Fig 8a). However, as soon as one of the expression level of the proteins changed, harmonic oscillations occurred. A change in the value of the protein initial level expression was translated by a change in the order of the oscillations (change of phase) (Fig 8b and 8c).

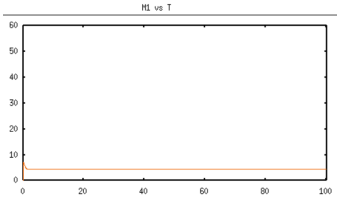

(a) $p_1(0) = p_2(0) = p_3(0)$

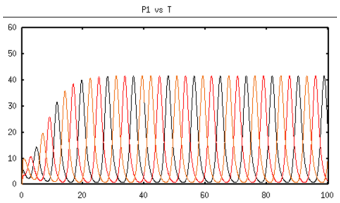

(b) $p_1(0) = 1$, $p_2(0) = p_3(0) = 0$

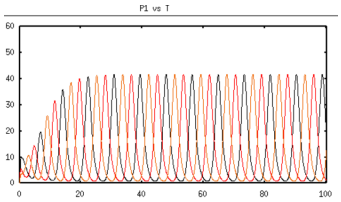

(c) $p_1(0) = p_3(0)$, $p_2(0) = 1$

Figure 8: Time plots of the protein expression of the repressilator with different initial conditions, p_1 in black, p_2 in red and p_3 in orange

2.1.1 The α_1, α_2 and α_3 parameters

These three alpha parameters represent the production rates of the messenger RNA (m). We simulated only the α_1 but the other two α behave in the same way as the three mRNAs are symmetric.

When all α are equal, the system produces harmonic oscillations (Fig 9a). When this parameter is reduced, the inhibition on the m_2 is lowered but the inhibition by p_2 on m_3 is increased consequently, as the concentration of p_2 is also increased (Fig 9b). In the inverse situation, when α_1 is increased, the amount of p_1 and p_3 is increased and p_2 is reduced, as the inhibition on m_2 is increased a,d subsequently the inhibition on m_3 by p_2 is reduced (Fig 9c). These observations were also confirmed by the bifurcation diagram of p_1 and p_2 in function of α_1 (Fig 9d) and 9e).

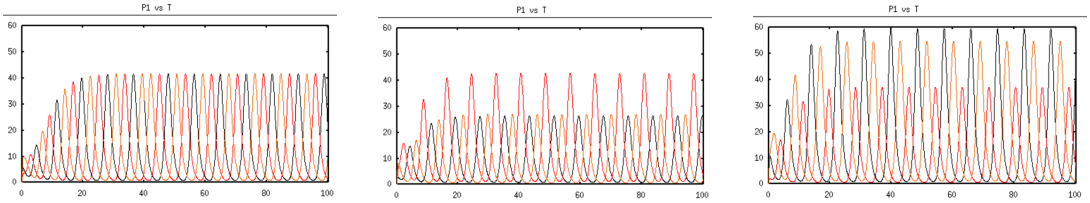

(a) $\alpha_1 = 100$ (b) $\alpha_1 = 50$ (c) $\alpha_1 = 200$

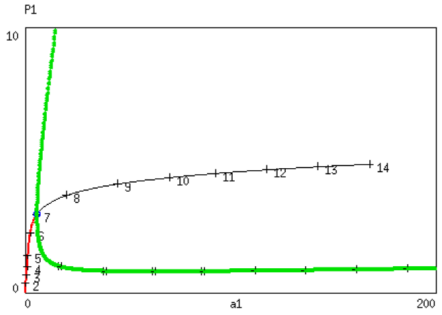

(d) Bifurcation diagram of p_1 in function of the parameter α_1

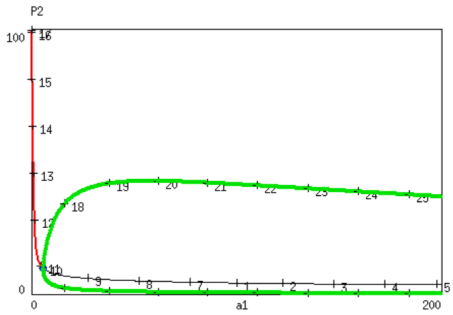

(e) Bifurcation diagram of p_2 in function of the parameter α_1

Figure 9: Impact of α_1 on the behaviour of the system, p_1 in black, p_2 in red and p_3 in orange

2.1.2 The α_0 parameter

This parameter is the number of mRNA created despite the presence of inhibitor on the promoter site of the protein gene. This means that if α_0 is different from 0, the protein is expressed, even if the promoter site of the gene is saturated with inhibitors.

We drew the stability diagram for α_1 and β with different values of α_0. When no mRNA is created in presence of inhibitors, the region for the oscillations is wide (Fig 10a), but when some mRNA can be transcribed despite the presence of inhibitors, the range of the region is reduced (Fig 10b). This means you need to compensate the values of the translation rate (β) and the production rate of the mRNA ($\alpha_{1,2,3}$) to compensate the continuous transcription of mRNA.

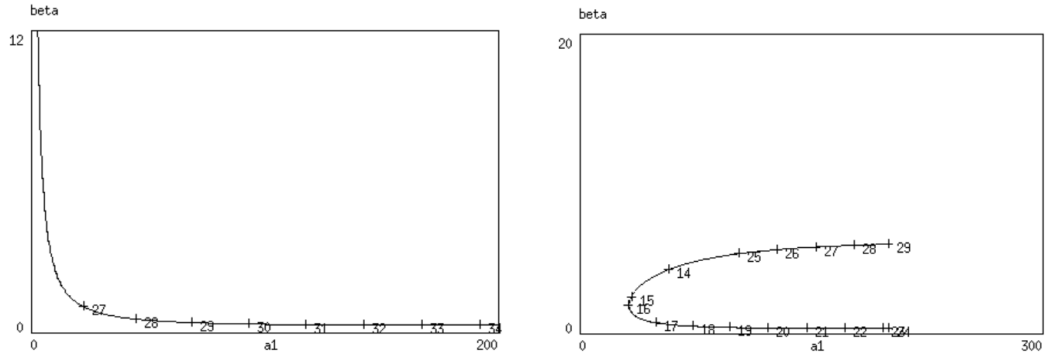

(a) $\alpha_0 = 0$ (b) $\alpha_0 = 1$

Figure 10: Stability diagram of the parameters α_1 and β with different values of α_0

2.1.3 The β and δ parameters

In the paper, the translation rate (β) and the degradation rate of the protein (δ) are assumed to be equal. To see if this is a necessary condition for harmonic oscillations, we drew a stability diagram of the two parameters (Fig 11a). Below the curve, the values of the parameters correspond to a system with harmonic oscillations, whereas above the curve we observe damped oscillations, corresponding to a stable focus (Fig 11b).

This means that assuming $\beta = \delta$ does not suffice as a condition for the harmonic oscillations, as we saw with the stability diagram that these are observed within a specific range of values.

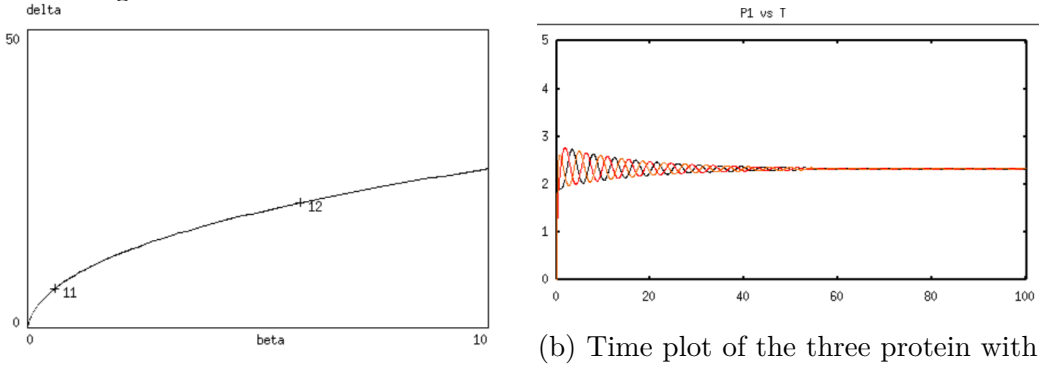

(a) Stability diagram of β and δ

(b) Time plot of the three protein with $\beta = 3$ and $\delta = 20$

Figure 11: Study of the impact of β and δ parameters on the behaviour of the system

2.2 Effect on the period

We can see that the value of some parameters have a greater effect on the period than the others. The α_0 parameter does not affect greatly the period beyond a slight increase beyond small values. However, the parameter δ, the degradation rate of the protein, affects it greatly. this could be explained by the fact that if the protein degrades quickly, the period of the oscillations will decrease as there is no longer protein to affect the other transcription sites.

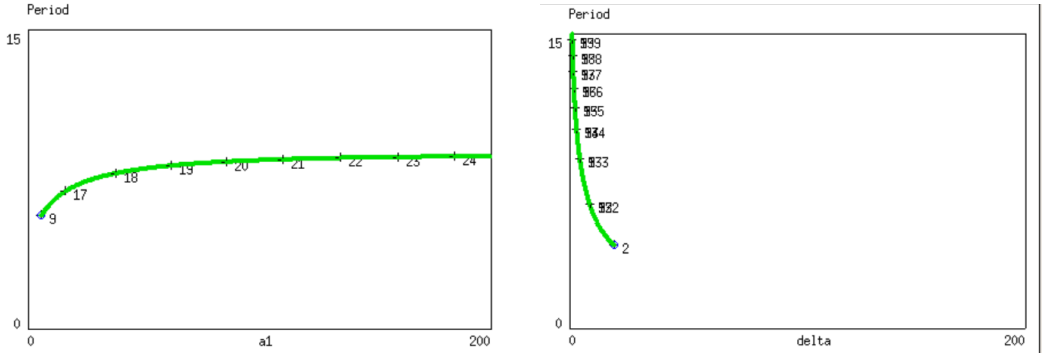

(a) Value of the period in function of α_0 (b) Value of the period in function of δ

Figure 12: Effect on the period in function of the parameters α_0 and δ

2.3 IPTG effect

To incorporate the IPTG inhibition on LacI, we reproduce the equation of the IPTG effect in the Toggle Switch (equation 2) into the equation of m_2 which correspond to the protein TetR possessing the promoter suppressed by LacI (equation 4).

$$\frac{dm2}{dt} = \alpha_2 \frac{K_2^n}{K_2^n + \left(\frac{p_1}{(1+S/K_s)^m}\right)^n} + \alpha_0 - \gamma m_2 \tag{9}$$

Default parameters : $K_s = 5, m = 2$

When the concentration of IPTG is constant, we observed at first a diminution of the amplitude of the oscillations of p_3, a consequence of the augmentation of p_2 as the inhibitory effect of p_1 is diminished because of the IPTG (Fig 13a). The higher the concentration of IPTG, the more the oscillations are damped until we reached the steady state without oscillation (Fig 13b and 13c). So in function of

the concentration of the IPTG, we passed from a limit cycle to a stable focus and finally a stable node.

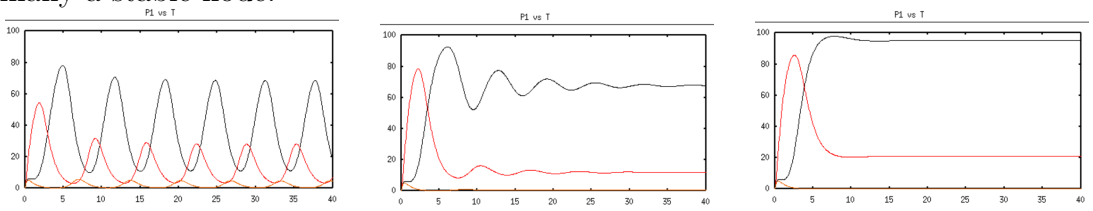

(a) $S = 10$ (b) $S = 20$ (c) $S = 30$

Figure 13: Time plots of the protein expression of the repressilator with different concentration of IPTG, p_1 in black, p_2 in red and p_3 in orange

The same phenomena can be observed with only a pulse of IPTG. However, as soon as the pulse is finished, the system returned to harmonic oscillations (Fig 14).

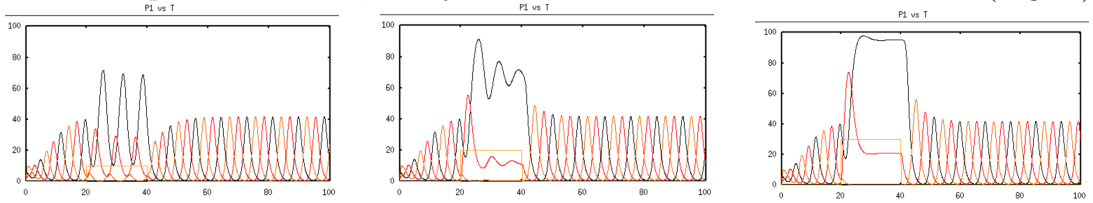

(a) $S = 10$ (b) $S = 20$ (c) $S = 30$

Figure 14: Time plots of the protein expression of the repressilator with a pulse of IPTG of different concentrations

2.4 GFP expression level

In the paper, they use GFP expression, inhibited by TetR, to mesure the level expression of the whole system. So conceptually, the level expression of GFP is equal to the expression of p_3, or λ cl. To write the equation of the GFP expression, we use then the equation of p_3 (equation 5).

$$\frac{dm_{GFP}}{dt} = \alpha_3 \frac{K_3^n}{K_3^n + p_2^n} + \alpha_0 - \gamma_{GFP} * m_{GFP} \tag{10}$$

$$\frac{dp_{GFP}}{dt} = \beta m_{GFP} - \delta_{GFP} * p_{GFP} \tag{11}$$

One figure of the same paper (Fig 15a) shows that GFP expression accumulates. When we simulated the repressilator with a degradation rate of the protein lower

than the translation rate, we observed the same phenomenon, which is an increase of the average level of the GFP expression (Fig 15b). When the degradation rate is higher, we observe a reduction of the amplitude of the oscillation for p_{GFP} (Fig 15c).

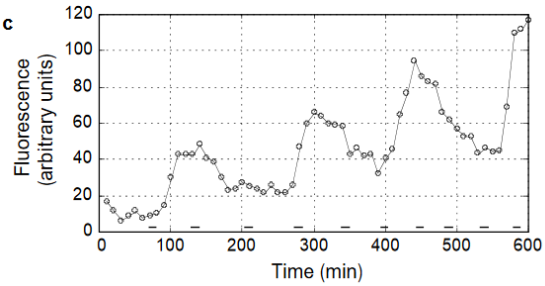

(a) Figure 2 of the article Elowitz and Leibler [2000], showing the average level expression of GFP

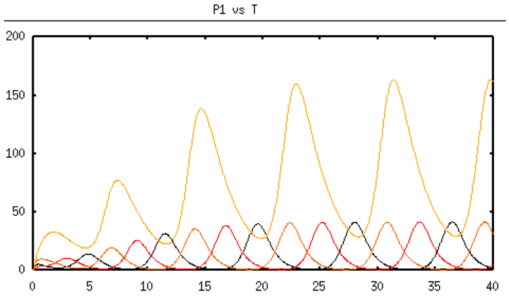

(b) $d_{GFP} = 2$

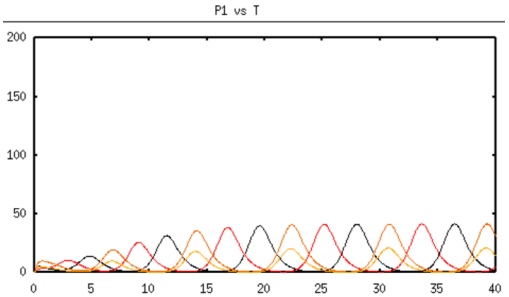

(c) $d_{GFP} = 10$

Figure 15: Time plots of the protein expression of the repressilator and the GFP expression, p_1 in black, p_2 in red, p_3 in orange and p_{GFP} in yellow

Part II
Stochastic simulations

3 Toggle Switch

Reaction step	Propensity
$\rightarrow X$	$\omega_1 = \alpha_1 \Omega \frac{K_1^n \Omega}{K_1^n \Omega + y^n}$
$X \rightarrow$	$\omega_2 = \delta_1 x$
$\rightarrow Y$	$\omega_3 = \alpha_2 \Omega \frac{K_2^n \Omega}{K_2^n \Omega + x^n}$
$Y \rightarrow$	$\omega_4 = \delta_2 y$

3.1 The effect of the size of the system

The Ω parameter defines the size of the system, particularly the number of molecules present. To observe the effect of the size of the system on the noise, we studied the variation of the value of one component, here X, around its mean for different values of Ω. We observed that when the system is small, the variation induced by the noise is high because we have only one molecule to observe. However, as the system grows in size, the noise is reduced because we look at a greater number of molecules. Indeed, the noise on one molecule is lost among all the other molecules. This is why we can observe a decrease of the noise in function of the increase of the system size (Fig 16).

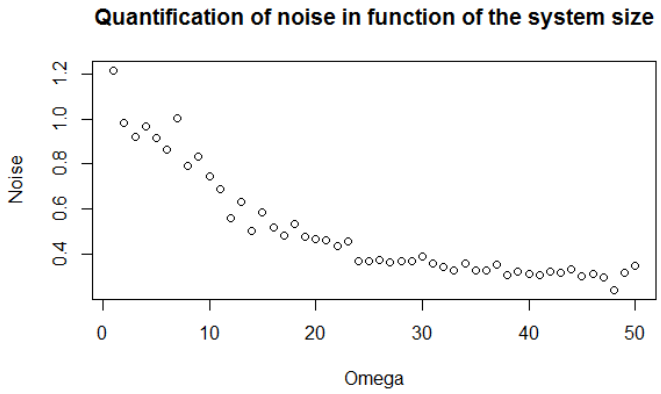

Figure 16: Noise obtained by running 30 times the Toggle Switch stochastic simulation and calculating the mean of their coefficient of variation for different size of the system (Omega)

3.2 Near the bistability domain

To find ourselves at the limit of the bistability domain, we chose a value for the α_1 parameter on the bifurcation diagram of this parameter in function of X. We chose $\alpha_1 = 1.507$ and as initial conditions $x_0 = 1$ and $y_0 = 0.5$.

We observed that X can be found in both its steady states from one simulation to another : in the higher one and in the lower one (Fig 17). This would not be possible in the deterministic model, as the initial condition would predict in which steady state we would be. The stochastic model allows the model to behave differently from one simulation to another, thus allowing us to observe both steady states with the same initial conditions.

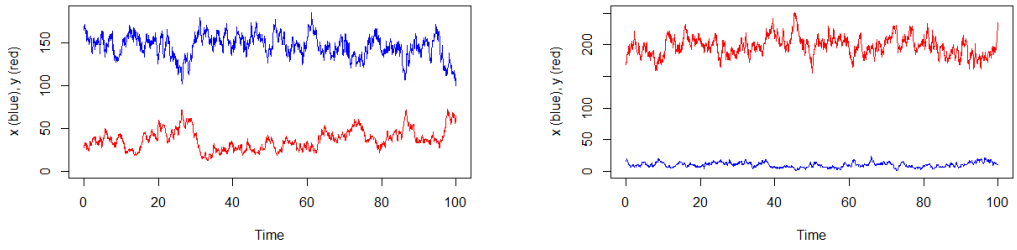

Figure 17: Time plots of X and Y at the limit of the bistability domain. We observe both steady states with the same initial conditions.

3.3 IPTG effect

We incorporated the IPTG in the X equation and simulated several times the time plot of X under the IPTG.

We observed that when we reduce the signal of the IPTG from 2 to 1, the time where the system switches greatly diverges, whereas at 2, the time of the switch was less distributed (Fig 18a and 18b).

For a signal of 0.8, we initially observed no switch. So we extended the time of exposure to the IPTG and observed sometimes a switch, but at very different time, which supports the theory of a switch more induced by the noise than by the IPTG (Fig 18c).

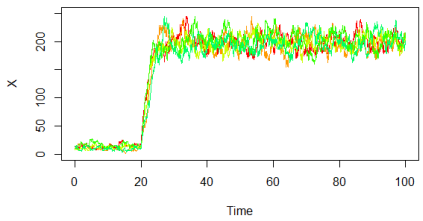

(a) $S = 2$ and the time = 60 seconds

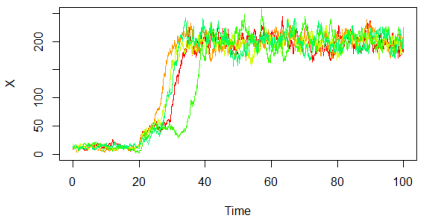

(b) $S = 1$ and the $time = 60seconds$

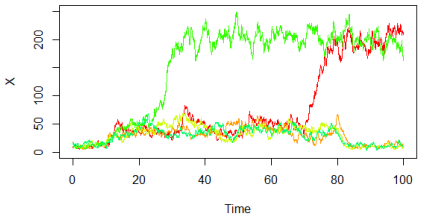

(c) $S = 0.8$ and the $time = 70seconds$

Figure 18: Time plots of the protein expression of the stochastic Toggle Switch system with different concentrations of IPTG

4 Repressilator

Reaction step	Propensity
$\rightarrow M_1$	$\omega_1 = \alpha_1\Omega\frac{K_1^n\Omega}{K_1^n\Omega+p_3^n} + \alpha_0\Omega$
$M_1 \rightarrow$	$\omega_2 = \gamma m_1$
$\rightarrow M_2$	$\omega_3 = \alpha_2\Omega\frac{K_2^n\Omega}{K_2^n\Omega+p_1^n} + \alpha_0\Omega$
$M_2 \rightarrow$	$\omega_4 = \gamma m_2$
$\rightarrow M_3$	$\omega_5 = \alpha_3\Omega\frac{K_3^n\Omega}{K_3^n\Omega+p_2^n} + \alpha_0\Omega$
$M_3 \rightarrow$	$\omega_6 = \gamma m_3$
$\rightarrow P_1$	$\omega_7 = \beta m_1$
$P_1 \rightarrow$	$\omega_8 = \delta p_1$
$\rightarrow P_2$	$\omega_9 = \beta m_2$
$P_2 \rightarrow$	$\omega_{10} = \delta p_2$
$\rightarrow P_3$	$\omega_{11} = \beta m_3$
$P_3 \rightarrow$	$\omega_{12} = \delta p_3$

4.1 The effect of the size of the system

As with the Toggle Switch stochastic model, we observe the same sensitivity to the noise when the system is small, that decreases when the system size increases (Fig 19).

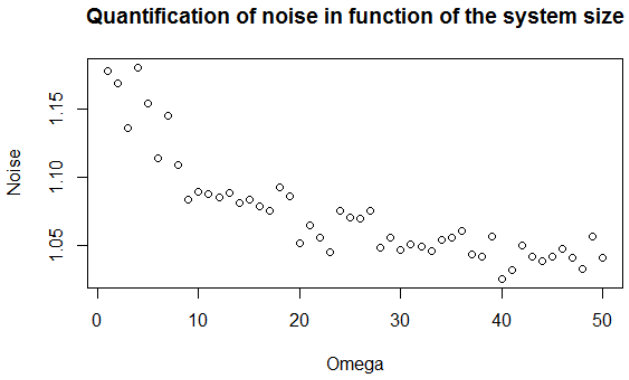

Figure 19: Noise obtained by running 5 times the Repressilator stochastic simulation and calculating the mean of their coefficient of variation for different size of the system (Omega)

4.2 On the limit cycle

To choose values for the limit cycle we ran a simulation on XPP then picked the values once the system was oscillating on the limit cycle. We then simulated with these values as initial conditions for the stochastic model with different values of Ω.

We can see with a little Ω the oscillations are unsynchronized almost immediatly, whereas with a high Ω the oscillations desyncrhonized only after at least three peaks (Fig 20).

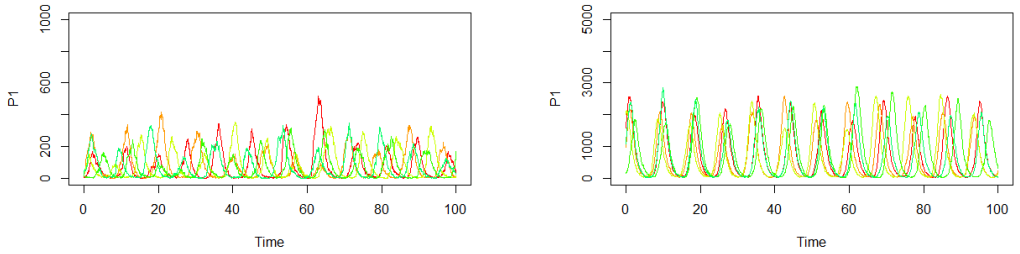

Figure 20: Time plots of p_1 with initial conditions on the limit cycle and $\Omega = 5$ (left) or $\Omega = 50$ (right)

4.3 IPTG effect

We incorporated the IPTG in the m_2 equation and run several times the simulation and represented each simulation of p_1 on a plot with different values for the signal of IPTG.

We observed that with a signal high enough ($S = 40$), the oscillations disappeared for the duration of the signal. With a lower signal ($S = 20$), we observed some small oscillations, ut with a considerably lower amplitude than observed without IPTG. We observed no inhibition whit a signal of 10. For both simulation, the cells were synchronized after the end of the pulse of IPTG (Fig 21).

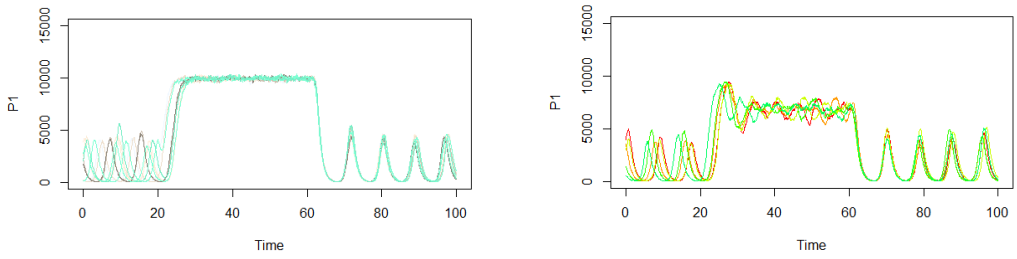

Figure 21: Time plots of p_1 with $S = 40$ (lef) and $S = 20$ (right)

References

Michael B. Elowitz and Stanislas Leibler. A synthetic oscillatory network of transcriptional regulators. *Nature*, 2000.

Timothy S. Gardner, Charles R. Cantor, and James J. Collins. Construction of a genetic toggle switch in escherichia coli. *Nature*, 2000.